British Journal of Pharmacology

DOI:10.1111/bph.13315
www.brjpharmacol.org

RESEARCH PAPER

Salsalate attenuates diet induced non-alcoholic steatohepatitis in mice by decreasing lipogenic and inflammatory processes

Correspondence
Anita van den Hoek, Department of Metabolic Health Research, TNO, Zernikedreef 9, 2333 CK Leiden, The Netherlands.
E-mail: a.vandenhoek@tno.nl

Received
23 March 2015
Revised
10 August 2015
Accepted
13 August 2015

Wen Liang[1,2], Lars Verschuren[3], Petra Mulder[1], José W.A. van der Hoorn[1], Joanne Verheij[4], Andrea D. van Dam[2], Mariette R. Boon[2], Hans M.G. Princen[1], Louis M. Havekes[1,2], Robert Kleemann[1] and Anita M. van den Hoek[1]

[1]Department of Metabolic Health Research, The Netherlands Organization for Applied Scientific Research (TNO), Leiden, The Netherlands, [2]Department of Endocrinology and Metabolic Diseases, Leiden University Medical Center, Leiden, The Netherlands, [3]Department of Microbiology and Systems Biology, TNO, Zeist, The Netherlands, and [4]Department of Pathology, Academic Medical Center, Amsterdam, The Netherlands

BACKGROUND AND PURPOSE

Salsalate (salicylsalicylic acid) is an anti-inflammatory drug that was recently found to exert beneficial metabolic effects on glucose and lipid metabolism. Although its utility in the prevention and management of a wide range of vascular disorders, including type 2 diabetes and metabolic syndrome has been suggested before, the potential of salsalate to protect against non-alcoholic steatohepatitis (NASH) remains unclear. The aim of the present study was therefore to ascertain the effects of salsalate on the development of NASH.

EXPERIMENTAL APPROACH

Transgenic APOE*3Leiden.CETP mice were fed a high-fat and high-cholesterol diet with or without salsalate for 12 and 20 weeks. The effects on body weight, plasma biochemical variables, liver histology and hepatic gene expression were assessed.

KEY RESULTS

Salsalate prevented weight gain, improved dyslipidemia and insulin resistance and ameliorated diet-induced NASH, as shown by decreased hepatic microvesicular and macrovesicular steatosis, reduced hepatic inflammation and reduced development of fibrosis. Salsalate affected lipid metabolism by increasing β-oxidation and decreasing lipogenesis, as shown by the activation of PPAR-α, PPAR-γ co-activator 1β, RXR-α and inhibition of genes controlled by the transcription factor MLXIPL/ChREBP. Inflammation was reduced by down-regulation of the NF-κB pathway, and fibrosis development was prevented by down-regulation of TGF-β signalling.

CONCLUSIONS AND IMPLICATIONS

Salsalate exerted a preventive effect on the development of NASH and progression to fibrosis. These data suggest a clinical application of salsalate in preventing NASH.

Abbreviations

ALT, alanine transaminase; AP-1, activator protein 1; AST, aspartate aminotransferase; Ccl2, chemokine (C-C motif) ligand 2; CETP, cholesteryl ester transfer protein; E3L, APOE*3Leiden; H&E, haematoxylin and eosin; HDL, high-density lipoprotein; HFC, high-fat and high-cholesterol diet; HOMA, homeostasis model assessment; IPA, Ingenuity Pathway Analysis; IL-6, interleukin 6; IR, insulin resistance; LDL, low-density lipoprotein; LFD, low-fat diet; MCP-1, monocyte chemotactic protein 1; MLXIPL/ ChREBP, MLX-interacting protein-like/carbohydrate response element binding protein; NAFLD, non-alcoholic fatty liver disease; NASH, non-alcoholic steatohepatitis; PGC1-β, PPAR-γ co-activator 1β; RXR-α, retinoid X receptor-α; TGF-β, transforming growth factor β; TIMP-1, TIMP metallopeptidase inhibitor 1; VLDL, very low-density lipoprotein

Tables of Links

TARGETS
Nuclear hormone receptors
PPAR-α
RXR-α, retinoid X receptor-α

LIGANDS
CCL2
IL-6
Salicylic acid
TGF-β
TIMP-1

These Tables list key protein targets and ligands in this article which are hyperlinked to corresponding entries in http://www.guidetopharmacology.org, the common portal for data from the IUPHAR/BPS Guide to PHARMACOLOGY (Pawson *et al.*, 2014) and are permanently archived in the Concise Guide to PHARMACOLOGY 2013/14 (Alexander *et al.*, 2013).

Introduction

Because of the worldwide epidemic of obesity and the abundance of energy-rich diets with high levels of sugars and saturated fat, the condition known as non-alcoholic fatty liver disease (NAFLD) is increasingly common. In fact, NAFLD is now considered to be the manifestation of the metabolic syndrome in the liver and has become the most prevalent form of chronic liver disease. Non-alcoholic steatohepatitis (NASH) is a severe form of NAFLD, characterized by steatosis in concert with inflammation, which can progress to liver fibrosis and cirrhosis. To date, no single therapy has been approved for the treatment of NASH. Considering that NASH has serious adverse effects on health, including hepatic failure, development of novel therapies that effectively reverse hepatic fat accumulation and inflammation, is clearly needed.

Salsalate (salicylsalicylic acid) is an anti-inflammatory agent that has been used clinically for several decades to treat rheumatoid arthritis, osteoarthritis and related rheumatic conditions. The drug consists of two molecules of salicylate that are linked by an ester bond. The anti-inflammatory effects of salsalate and salicylate are both believed to be attributable to inhibition of the activity of COX, a key enzyme in biosynthesis of pro-inflammatory prostanoids (Morris *et al.*, 1985; Xu *et al.*, 1999). In contrast to salicylate, salsalate is well tolerated and considered to be relatively safe for long-term use. For instance, salsalate exhibited beneficial effects on glucose and lipid metabolism. In clinical studies, administration of salsalate decreased fasting glucose and HbA1c levels in obese non-diabetics as well as type 2 diabetes, and improved insulin sensitivity (Koska *et al.*, 2009; Goldfine *et al.*, 2010). Furthermore, decreases in circulating triglyceride and free fatty acids have been reported (Goldfine *et al.*, 2008; Goldfine *et al.*, 2013b). In aggregate, these data led us to the hypothesis that this particular combination of effects, that is, anti-inflammatory effects and beneficial effects on glucose and lipid metabolism, render salsalate an optimal candidate for treatment of NASH.

To test this hypothesis, we investigated the effect of salsalate on NASH development and liver fibrosis using APOE*3Leiden.CETP (E3L.CETP) mice (Westerterp *et al.*, 2006; Zadelaar *et al.*, 2007; van den Hoek *et al.*, 2014). These mice are prone to develop dyslipidemia, obesity and NAFLD on a high-fat and high-cholesterol diet and ultimately develop NASH with fibrosis. Earlier studies have shown that these mice demonstrate human-like responses to different anti-diabetic and hypolipidemic drugs (van der Hoogt *et al.*, 2007; de Haan *et al.*, 2008; van der Hoorn *et al.*, 2008; Kuhnast *et al.*, 2014; van den Hoek *et al.*, 2014).

Methods

Animals and induction of NASH and liver fibrosis

All animal care and experimental procedures were approved by the Ethical Committee on Animal Care and Experimentation (Zeist, The Netherlands), and were in compliance with European Community specifications regarding the use of laboratory animals. All studies involving animals are reported in accordance with the ARRIVE guidelines for reporting experiments involving animals (Kilkenny *et al.*, 2010; McGrath *et al.*, 2010). A total of 42 animals were used in the experiments described here.

Homozygous human cholesteryl ester transfer protein (CETP) transgenic mice (strain 5203) (Jiang *et al.*, 1992; van den Hoek *et al.*, 2014) were obtained from Jackson Laboratories (Bar Harbor, ME, USA) and cross-bred with E3L mice (van den Maagdenberg *et al.*, 1993) in our local animal facility at TNO to obtain heterozygous E3L.CETP mice. All animals were housed in a temperature-controlled room on a 12 h light–dark cycle and had free access to food and water. Mice were killed by CO_2 inhalation.

To assess the effect of salsalate on progression of obesity, dyslipidemia, hyperglycaemia and NASH development, 16–19 weeks old male E3L.CETP mice were randomized on age, body weight, plasma cholesterol and triglycerides into the different groups and were fed a high-fat/high-cholesterol diet (HFC: 45 kcal% fat derived from lard Cat. no. 12451, supplemented with 1% (w/w) cholesterol; Research Diets, New Brunswick, NJ, USA) with (n = 8) or without (HFC control group, n = 9) 1% (w/w) salsalate (2-carboxyphenyl salicylate, TCI Europe N.V., Zwijndrecht, Belgium) for 12 weeks. In addition, five age-matched male E3L.CETP mice on a low-fat diet (LFD: 10 kcal% lard, Cat. no. 12450B, Research Diets) were also included (LFD control group, n = 5). In a second experiment, we assessed whether salsalate would still be able to

prevent onset of NASH and liver fibrosis, also after a longer induction period of NASH. To do so, 11–18 weeks old male E3L.CETP mice were randomized on age, body weight, plasma cholesterol and triglycerides into two groups and were fed the HFC diet with (n = 8) or without (n = 12) 0.33% (w/w) salsalate for 20 weeks. Because of the profound effects of salsalate in the first (12 week) study, the dose of salsalate in this 20 week study was reduced to a third of that used in the first study.

Analysis of plasma biochemical variables

Blood was collected from the tail vein after 5 h fasting (with food withdrawn around 08.00 h) into EDTA-coated tubes (Sarstedt, Nümbrecht, Germany). Plasma glucose was determined using the 'Freestyle glucose measurement system' from Abbott (Abbott Park, IL, USA). Plasma insulin was measured by ELISA (Mercodia AB, Uppsala, Sweden). Homeostasis model assessment (HOMA) was used to calculate relative insulin resistance (IR). Five hours fasting plasma insulin and fasting plasma glucose values were used to calculate IR, as follows: IR = [insulin (ng ml^{-1}) × glucose (mM)]/22.5. Plasma total cholesterol, triglycerides, ketone bodies, CCL2, the tissue inhibitor of metalloproteinases (TIMP-1), and IL-6 were determined using commercially available kits (cholesterol and triglycerides: Roche Diagnostics, Basel, Switzerland; ketone bodies: Instruchemie, Delfzijl, The Netherlands; CCL2 and TIMP-1: R&D Systems Inc, Minneapolis, MN, USA; IL-6: Life Technologies, Bleiswijk, The Netherlands). The distribution of cholesterol of various lipoproteins was determined in plasma pooled per group after separation of lipoproteins by fast-performance liquid chromatography using a Superose 6 column (van der Hoorn *et al.*, 2008). Plasma alanine transaminase (ALT) and aspartate aminotransferase (AST) were measured using a Reflotron® kit (Roche diagnostics). All assays were performed according to the manufacturers' instructions.

Histology

Liver samples (lobus sinister medialis hepatis and lobus dexter medialis hepatis) were collected (from non-fasted mice), fixed in formalin and paraffin embedded, and sections were stained with haematoxylin and eosin (H&E) and Sirius Red. NAFLD were scored in H&E-stained cross sections using an adapted grading system of human NASH (Kleiner *et al.*, 2005; Liang *et al.*, 2014). In short, the level of macrovesicular and microvesicular steatosis was determined at 40× to 100× magnification relative to the total liver area analysed and expressed as a percentage. Inflammation was scored by counting the number of aggregates of inflammatory cells per field using a 100× magnification (view size of 3.1 mm^2). The average of five random fields was taken. Relative values against the average of the HFC control group were calculated. Hepatic fibrosis was identified using Sirius Red stained slides and evaluated using an adapted grading system of human NASH (Kleiner *et al.*, 2005; Tiniakos *et al.*, 2010), in which the presence of pathological collagen staining was scored as either absent (0), observed within perisinusoidal/perivenular or periportal area (1), within both perisinusoidal and periportal areas (2), bridging fibrosis (3) or cirrhosis (4). Furthermore, the level of collagen deposition in the perisinusoidal area was determined relative to the total perisinusoidal area analysed, expressed as a percentage. In addition, fibrosis was quantified by measuring the hydroxyproline (as a measure for collagen) and proline (as a measure for total protein) content of liver tissue using HPLC as previously described (Bank *et al.*, 1997) and subsequent calculation of the ratio hydroxyproline : proline.

Hepatic lipid analysis

Liver samples of lobus sinister lateralis hepatis were collected, and the intrahepatic concentration of triglycerides, free cholesterol and cholesteryl esters was determined as described previously (van der Hoogt *et al.*, 2007). Approximately 50 mg of tissue was homogenized in PBS, and samples of the homogenate were taken for measurement of protein content. Lipids were extracted and separated by high performance thin layer chromatography on silica gel plates. Lipid spots were stained with colour reagent (5 g $MnCl2.4H_2O$, 32 mL 95–97% H_2SO_4 added to 960 mL of CH_3OH:H_2O 1:1 v/v) and quantified using TINA® version 2.09 software (Raytest, Straubenhardt, Germany).

RNA isolation and microarray analysis

Nuclear acid extraction was performed as described previously in detail (Verschuren *et al.*, 2014). Briefly, total RNA was extracted from individual liver samples (n = 9 liver samples for HFC control group and n = 8 liver samples for salsalate-treated group) using glass beads and RNAzol (Campro Scientific, Veenendaal, The Netherlands). RNA integrity was examined using the RNA 6000 Nano Lab-on-a-Chip kit and a bioanalyzer 2100 (Agilent Technologies, Amstelveen, The Netherlands). The Illumina® TotalPrep™ RNA amplification kit (Ambion, art. no. AM-IL1791) was used to synthesize biotin-labelled cRNA starting with 500 ng total RNA. The concentration of the labelled cRNA was measured using the Nanodrop spectrophotometer. The amount of biotinylated cRNA, which was hybridized onto the MouseRef-8 Expression BeadChip, was 750 ng. Illumina's Genomestudio v1.1.1 software with the default settings advised by Illumina was used for gene expression analysis. All the quality control data of this BeadChip were within specifications of the microarray service provider (Service XS, Leiden, The Netherlands).

The probe-level, background-subtracted, expression values were used as input for lumi package (Du *et al.*, 2008) of the R/Bioconductor (http://www.bioconductor.org; http://www.r-project.org) to perform quality control and a quantile normalization. Unexpressed probes ($P > 0.01$) were removed from further analysis, and 12 947 probes remained in the analysis. Differentially expressed probes were identified using the limma package of R/Bioconductor (Smyth, 2004; Verschuren *et al.*, 2014) calculated values of $P < 0.001$ were used as threshold for significance. Selected differentially expressed probes were used as an input for pathway analysis through Ingenuity Pathway Analysis (IPA) suite (www.ingenuity.com, accessed 2014).

Upstream regulator analysis was performed using the IPA software (Kramer *et al.*, 2014). This analysis determines the activation state of transcription factors based on the observed differential gene expression. This results in an overlap P-value and activation z-score for each transcription factor in the IPA knowledge base. The overlap P-value indicates the

significance of the overlap between the known target genes of a transcription factor and the differentially expressed genes measured in an experiment. The activation z-score indicates activation (positive z-score) or inhibition (negative z-score) of a particular transcription factor. An activation z-score <-2 or >2 indicates significant inhibition or activation of a pathway or process.

Gene expression analysis by RT-PCR

To confirm the gene expression data of the microarray analysis gene expression of selected genes was measured via RT-PCR. To generate cDNA for RT-PCR, cDNA was synthesized from 1 μg of RNA using a high capacity RNA-to-cDNA™ Kit (Life Technologies, Bleiswijk, The Netherlands). RT-PCR was performed in duplicate on a 7500 fast real-time PCR machine. TaqMan® gene expression assays (Life Technologies) were used to detect expression of SREBP-1c (Srepf1, Mm00550338_m1), FASN (Mm00662319_m1), SCD-1 (Mm00772290_m1), PPARα (Mm00440939_m1), CD68 (Mm03047340_m1), Ccl2 (Mm00441242_m1), Tnf-α (Tnf, Mm00443258_m1), IL-6 (Mm00446191_m1), αSMA (Acta2, Mm01546133_m1), Col1a1 (Mm00801666_g1), TIMP-1 (Mm01341358_m1) and TGF-β (Tgfb1, Mm00441724_m1). Peptidylprolyl isomerase F (Ppif; Mm00506384_m1) was used as endogenous control. Changes in gene expression were calculated using the comparative Ct (ΔΔCt) method and expressed as fold-change relative to LFD.

Data analysis

All values shown represent means ± SEM. Statistical differences between groups were determined by using the non-parametric Mann–Whitney *U*-test for independent samples. Values of $P<0.05$ were considered statistically significant.

Results

Salsalate prevents weight gain and improves glycemic control and hyperlipidemia

To induce obesity, insulin resistance and hyperlipidemia, E3L.CETP mice were fed a HFC diet for 12 weeks. The HFC feeding resulted in an increased body weight (with 45%, $P < 0.01$) and elevated plasma insulin (8.0-fold, $P < 0.001$), cholesterol (4.1-fold $P < 0.001$) and triglyceride levels (2.7-fold, $P < 0.01$) when compared with age-matched control E3L.CETP mice on LFD, while plasma glucose levels remained similar (Table 1). The HFC diet led to an increased liver weight (2.0-fold, $P < 0.01$), and analysis of liver enzymes showed a concomitant increase in plasma ALT (8.9-fold, $P < 0.001$) and AST (3.6-fold, $P < 0.001$) as compared with the LFD mice, indicating that the HFC diet caused liver damage (Table 1).

Salsalate treatment profoundly curtailed weight gain, resulting in a significantly lower body weight after 12 weeks of treatment as compared with the HFC control group (with −41%, $P < 0.001$; Table 1). This decrease was at least partly due to a lower fat mass as reflected by a decrease in perigonadal fat pad weight with salsalate (with −83%, $P < 0.001$, data not shown). Fasting plasma glucose and insulin levels were significantly lower as compared with HFC control group after treatment with salsalate (with −36% and −89%, respectively, both $P < 0.01$; Table 1). Salsalate significantly decreased insulin resistance as reflected by the HOMA index (with −91%, $P < 0.01$), normalizing it to similar levels as age-matched control mice on LFD. Plasma lipids were also improved by salsalate treatment. More specifically, salsalate significantly decreased plasma cholesterol and triglycerides as compared with the HFC control group (with −72% and −91%, respectively, both $P < 0.001$; Table 1), mainly due to a reduction in very low-density lipoprotein (VLDL) and low-density lipoprotein (LDL), while high-density lipoprotein (HDL) cholesterol was slightly increased (Figure 1). Furthermore, liver weight, plasma ALT and AST were all significantly lower in the salsalate-treated groups as compared with the HFC control group (with −37%, −73% and −64%, respectively, all $P < 0.001$; Table 1).

Salsalate prevents hepatic steatosis and inflammation

NASH development was histologically evaluated using H&E and Sirius Red stained liver cross sections. HFC feeding induced pronounced steatosis, while treatment with salsalate fully prevented this induction resulting in a similar histological appearance as observed in the LFD group (Figure 2A). Quantitative analysis revealed that in the HFC group about 85% of the surface area was steatotic, of which 60% consisted of microvesicular steatosis and 25% of macrovesicular steatosis (Figure 2B, C). Treatment with salsalate completely prevented the development of microvesicular and macrovesicular steatosis (resulting in an average surface area of 0.1% and 0%, respectively, both $P < 0.001$). Biochemical analysis of intrahepatic liver lipids was in line with the histological analysis and revealed that HFC feeding resulted in a significant increase in hepatic triglycerides and cholesterol esters as compared with the LFD control group (5.1-fold and 4.1-fold, respectively, both $P < 0.01$, Figure 2D, E) and tended to increase free cholesterol as well (1.6-fold, $P = 0.065$; Figure 2F). Salsalate treatment normalized the intrahepatic lipids, resulting in significantly lower levels of hepatic triglycerides, cholesterol esters and free cholesterol as compared with the HFC group (6.7-fold, 3.2-fold and 2.4-fold decrease, respectively, all $P < 0.001$). HFC feeding also induced lobular inflammation, characterized by the presence of mononuclear cells and polymorphonuclear cells that formed aggregates, while the livers of the salsalate-treated mice contained scarcely any inflammatory aggregates (Figure 2A). Quantification of lobular inflammation showed that the HFC feeding resulted in a significant increase in the number of aggregates as compared with the LFD control group (8.0-fold, $P < 0.001$). Salsalate treatment fully blunted this HFC-induced inflammation, as shown by a significantly lower number of inflammatory aggregates relative to HFC group (10.2-fold decrease, $P < 0.001$; Figure 2G). Twelve weeks of HFC feeding induced onset of fibrosis, as shown by the patches of collagen deposition (Figure 2A; Sirius Red staining). Fibrosis evaluation according to human grading system revealed that some fibrosis was located within perisinusoidal and periportal area for all groups (score F2 for all groups). No bridging fibrosis was seen. However, the amount of perisinusoidal fibrosis (expressed as a percentage) significantly differed between

Table 1

Effects of diet and salsalate on biochemical variables in plasma from E3L.CETP mice

	LFD	HFC	HFC + S
Body weight (g)	33.8 ± 1.9	49.0 ± 1.4$^{\#}$	28.9 ± 1.1*$^{\#}$
Plasma glucose (mM)	12.6 ± 0.8	13.1 ± 0.7	8.4 ± 0.7*$^{\#}$
Plasma insulin (ng·mL^{-1})	0.6 ± 0.2	4.8 ± 0.7$^{\#}$	0.5 ± 0.2*
HOMA	0. ± 0.1	2.8 ± 0.4$^{\#}$	0.2 ± 0.1*
Plasma cholesterol (mM)	6.5 ± 1.0	26.9 ± 1.9$^{\#}$	7.5 ± 0.4*
Plasma triglycerides (mM)	2.6 ± 0.3	7.2 ± 1.0$^{\#}$	0.6 ± 0.05*$^{\#}$
Liver weight (g)	1.6 ± 0.1	3.2 ± 0.2$^{\#}$	2.0 ± 0.1*$^{\#}$
Plasma ALT (U/L)	32.2 ± 7.5	286.6 ± 53.5$^{\#}$	77.4 ± 9.2*$^{\#}$
Plasma AST (U/L)	131.8 ± 18.3	473.7 ± 70.5$^{\#}$	173.0 ± 9.3*

Body weight, liver weight and plasma parameters in APOE*3Leiden.CETP mice fed a low-fat diet (LFD; $n = 5$), a high-fat and high-cholesterol diet (HFC; $n = 9$) or a high-fat and high-cholesterol diet supplemented with salsalate (HFC + S; $n = 8$). *$P < 0.05$ significantly different from HFC; $^{\#}P < 0.05$ significantly different from LFD; Mann-Whitney *U*-test.

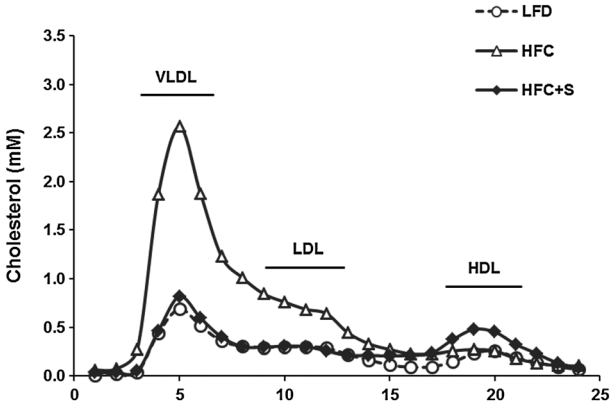

Figure 1

Lipoprotein profile. Lipoprotein profiles of APOE*3Leiden.CETP mice fed a low-fat diet (LFD; $n = 5$), a high-fat and high-cholesterol diet (HFC; $n = 9$) or an HFC diet supplemented with salsalate (1% w/v; HFC + S; $n = 8$) for 12 weeks. The distribution of cholesterol over the individual lipoprotein profiles in pooled plasma was determined after separation of lipoprotein profiles by fast-performance liquid chromatography.

groups and was significantly reduced in the salsalate-treated group as compared with HFC group (7.5-fold decrease, $P < 0.05$; Figure 2H).

Salsalate affects expression of genes involved in lipid metabolism, inflammation and energy metabolism

To further investigate the mechanism by which salsalate affects NASH development, transcriptome analysis of liver tissue was performed. Genes that were differentially expressed in the salsalate-treated group relative to the HFC control group were used for analysis of biological processes (n = 4514, of which 2356 genes were up-regulated, and 2158 genes were down-regulated by salsalate). Enrichment analysis identified 70 biological process categories that were significantly changed by salsalate. A subset of these biological process categories, including several with relevance to NASH development, is shown in Figure 3A. The categories 'Lipid Metabolism', 'Inflammatory Response', 'Energy Production' and 'Connective Tissue Disorders' were found to be predominantly affected by salsalate treatment. We subsequently analysed these four processes each in more detail by performing an upstream regulator analysis that determines the activation state (z-score) of the transcription factors involved, based on the changes in expression of their target genes. For each category, the transcription factors that significantly affect a pathway and have relevance to NASH development are shown in Table 2. The gene expression data of the microarray analysis was confirmed by analysing the gene expression of selected genes involved in fatty acid metabolism, inflammation or fibrosis by RT-PCR (Figure 4A–C).

The transcriptomics analysis revealed that salsalate affected lipid metabolism by increasing β-oxidation, as shown by the activation of PPAR-α, PGC1-β and RXR-α-controlled genes. Especially PPAR-α is one of the most important transcription factors in lipid metabolism and activation promotes uptake and utilization of fatty acids by upregulation of genes involved in fatty acid transport, binding and activation, and peroxisomal and mitochondrial fatty acid β-oxidation. The increase of β-oxidation by salsalate was supported by significantly higher ketone bodies measured after 20 weeks of treatment in the second experiment (0.03 ± 0.01 mM vs. 0.2 ± 0.2 mM for HFC and HFC + S, respectively, $P < 0.001$, data not shown). Furthermore, salsalate inhibited lipogenesis as shown by the inhibition of MLXIPL/ChREBP, the major transcription factor for activation of triglyceride synthesis.

Inflammation was evidently inhibited by salsalate, because almost all transcription factors in the inflammatory response process were found to be inactive when compared with HFC. The anti-inflammatory role of salsalate was confirmed by measurement of the inflammatory chemokine Ccl2 (MCP-1) in plasma after 12 weeks of treatment in the

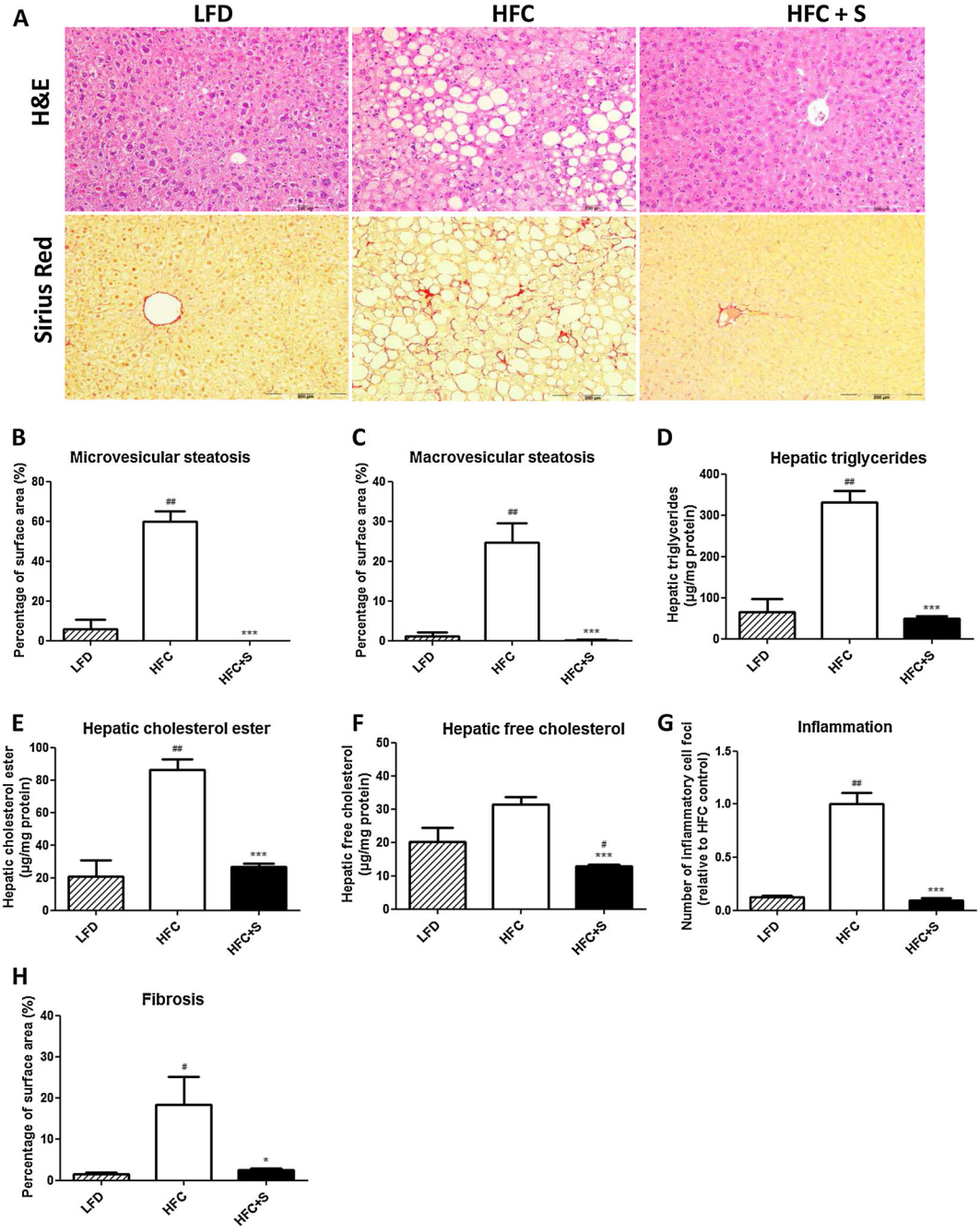

Figure 2

Histological photomicrographs and quantitative analysis of NASH in mice. Liver histological cross sections (A) and quantitative analysis (B–H) from APOE*3Leiden.CETP mice fed a low-fat diet (LFD; $n = 5$), a high-fat and high-cholesterol diet (HFC; $n = 9$) or an HFC diet supplemented with salsalate (HFC + S; $n = 8$) for 12 weeks. Upper photomicrographs: haematoxylin and eosin (H&E); lower photomicrographs: Sirius Red staining; magnification 200×. Microvesicular (B) and macrovesicular (C) steatosis as percentage of total liver area, intrahepatic triglycerides (D), intrahepatic cholesterol esters (E) and intrahepatic-free cholesterol (F), inflammatory foci per microscopic field (G) and fibrosis score (H) were analysed. *$P < 0.05$, ***$P < 0.001$, significantly different from HFC; #$P < 0.05$, ##$P < 0.01$, significantly different from LFD; Mann-Whitney *U*-test.

first experiment (Figure 4E). Plasma IL-6 levels were not affected by salsalate (Figure 4D), which is in line with the hepatic gene expression of IL-6 (Figure 4B). The NF-κB pathway plays a central role in NASH development, and the involved transcriptional regulators were clearly inhibited by salsalate treatment.

Most of the transcription factors in energy production were activated, and in general, the effects of salsalate were directed at mitochondrial activation and peroxisomal and mitochondrial β-oxidation.

We also performed an upstream regulator analysis for the process 'Connective Tissue Disorders', because this might

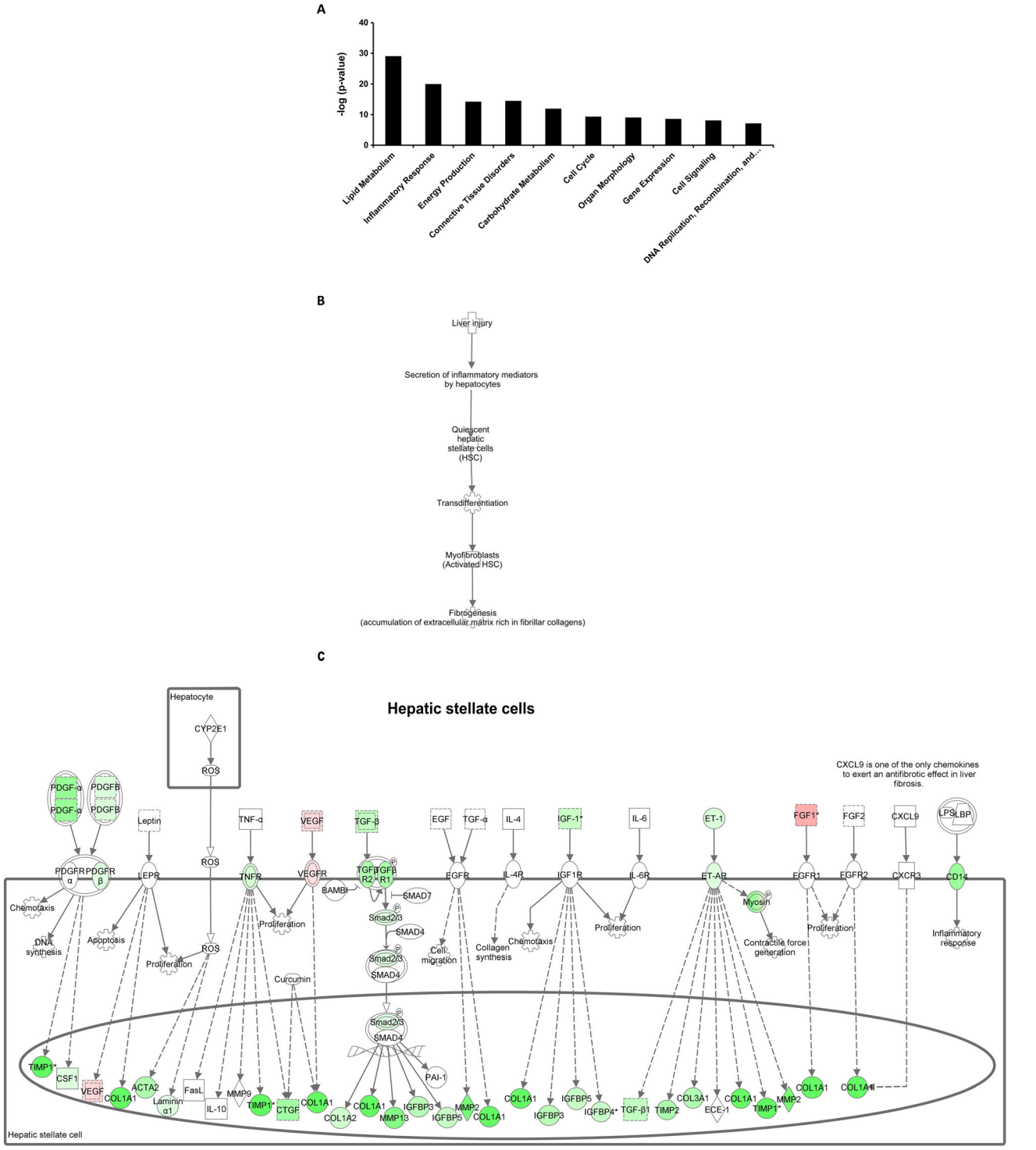

Figure 3

Enriched biological processes and hepatic fibrosis pathway analysis. A selection of significantly enriched biological processes (-log (*P*-value)) (A) and the sequence of events leading to fibrosis (B) and pathway analysis showing statistically significant gene expression changes in hepatic stellate cells (C) of APOE*3Leiden.CETP mice fed a HFC diet supplemented with salsalate for 12 weeks ($n = 8$) relative to HFC diet fed control group ($n = 9$). Red colour indicates up-regulation and green colour indicates down-regulation.

provide more insight in pathways contributing to the development of hepatic fibrosis. Salsalate inhibited most transcription factors in this category, including AP-1, an important regulator of differentiation, proliferation and apoptosis. The anti-fibrotic role of salsalate was confirmed by measurement of the collagenase inhibitor TIMP-1 in plasma after 12 weeks

Table 2

Hepatic gene expression

Upstream regulator	Activation z-score	*P*-value of overlap	Function
Lipid metabolism			
PPARA	5.567	2.65E-86	Major regulator of lipid metabolism
PPARGC1B	2.724	7.19E-11	Involved in fat oxidation
RXRA	2.417	1.93E-35	Required for PPARA transcriptional activity on fatty acid oxidation genes
ESRRA	2.215	1.73E-11	Regulator of gluconeogenesis and fatty acid metabolism
NR5A2	2.065	2.34E-08	Regulator of cholesterol and bile acid metabolism
MLXIPL	–2.194	3.82E-05	Activator of triglyceride synthesis
SERTAD2	–2.000	4.43E-04	Modulates fat storage by down-regulating adipocyte lipolysis
Inflammatory response			
NFkB (complex)	–6.676	1.40E-43	Key regulator of immune and inflammatory responses
NFKB1	–3.427	1.46E-29	DNA binding subunit of the NFkB protein complex
NFATC2	–3.313	5.31E-11	Pays a central role in inducing gene transcription during the immune response
IRF1	–3.252	1.33E-15	Regulator of immune response, apoptosis and DNA damage
NFKBIA	–3.186	4.70E-32	Inhibitor of NFkB
REL	–3.064	5.83E-12	Important role in B-cell survival and proliferation
CEBPD	–2.883	1.54E-10	Regulator of immune and inflammatory responses
RELA	–2.862	8.80E-36	Involved in NFκB heterodimer formation, nuclear translocation and activation
Nfat (family)	–2.611	1.09E-03	Family of transcription factors important in immune response
USF2	–2.567	6.67E-05	Binds to a symmetrical DNA sequence that is found in viral and cellular promoters
SQSTM1	–2.566	1.93E-06	Activator of the NFkB signaling pathway
STAT1	–2.175	4.63E-25	Important for cell viability in response to different cell stimuli and pathogens
Energy production			
PPARA	4.788	4.19E-39	Regulates the peroxisomal beta-oxidation pathway of fatty acids
INSR	4.588	1.33E-23	Insulin receptor that plays a key role in the regulation of glucose homeostasis
ESRRA	3.069	9.85E-16	Regulator of mitochondrial biogenesis and oxidative phosphorylation
PPARGC1A	2.729	6.67E-19	Regulator of mitochondrial biogenesis and function.
PPARGC1B	2.592	1.65E-08	Involved in non-oxidative glucose metabolism and energy expenditure
FOXO1	2.400	1.89E-09	Regulator of gluconeogenesis and glycogenolysis by insulin signaling
PCK1	–2.646	2.94E-13	Main control point for the regulation of gluconeogenesis
SERTAD2	–2.000	2.08E-06	Inhibitor of thermogenesis and oxidative metabolism
Connective tissue disorders			
SMAD7	2.054	9.33E-12	Inhibitor of TGF-β signaling
TGFB1	–3.838	2.90E-52	Controls cell growth, cell proliferation, cell differentiation and apoptosis
SMAD3	–2.758	1.12E-11	Regulator of TGF-β mediated transcription
STAT3	–2.558	6.13E-17	Key regulator for cell growth and apoptosis
Ap1	–2.373	2.75E-14	Regulator of differentiation, proliferation, and apoptosis

Effect of salsalate on hepatic gene expression involved in lipid metabolism, inflammatory response, energy production and connective tissue disorders. APOE*3Leiden.CETP mice received a high-fat and high-cholesterol diet with ($n = 8$) or without ($n = 9$) salsalate for 12 weeks. Data represent predicted activation state (z-score) of the upstream regulators, based on the expression changes of known target genes. The overlap *P*-value indicates the significance of the overlap between the known target genes of a transcription factor and the differentially expressed genes measured in an experiment. Red colour indicates up-regulation, and green colour indicates down-regulation.

of treatment in the first experiment (Figure 4F). Moreover, salsalate inhibited TGF-β signalling. TGF-β stimulates the proliferation and activation of fibroblasts, which deposit connective tissue and plays an important role in fibrosis. To investigate the effects of salsalate on expression of genes pertaining to the sequence of events leading to fibrosis in more detail, a pathway analysis was performed. The significant expression changes upon salsalate treatment in genes belonging to generic sequence of events from liver injury to fibrogenesis (Figure 3B) were analysed and demonstrate the cell specific down-regulation of fibrogenic genes in the liver. More specifically, the early signalling events in hepatic stellate cells (Figure 3C), containing PDGF, TGF-β, insulin growth factor-1 and endothelin-1 and associated downstream factors were down-regulated by salsalate. Furthermore, also in already activated stellate cells, salsalate was able to down-regulate genes involved in fibrogenesis (Figure 5). All together, these expression changes unambiguously show a profound down-regulation of the fibrogenesis pathway, following treatment with salsalate.

Salsalate prevents hepatic fibrosis

In a second experiment, the HFC induction period of NASH was prolonged (to 20 weeks) to evaluate whether salsalate would still be able to prevent onset of NASH and liver fibrosis, also after a longer duration of metabolic overload. Again, salsalate treatment led to a significantly lower body weight, plasma insulin, cholesterol and triglycerides levels as compared with the HFC control group (with −26%, −81%, −45% and −76%, respectively, all $P < 0.01$; data not shown). Histological evaluation of the liver confirmed the results of the first experiment and demonstrated that salsalate attenuated NASH development in this experiment as well, even after the longer NASH induction period and at the lower dose used (Figure 6A). Quantitative analysis showed that microvesicular steatosis and macrovesicular steatosis were significantly lower in the salsalate-treated group as compared with the HFC group (with 86%, $P < 0.05$ and 98%, $P < 0.001$, respectively; Figure 6B, C). Also, lobular inflammation, quantified as the number of inflammatory aggregates, was significantly reduced in the

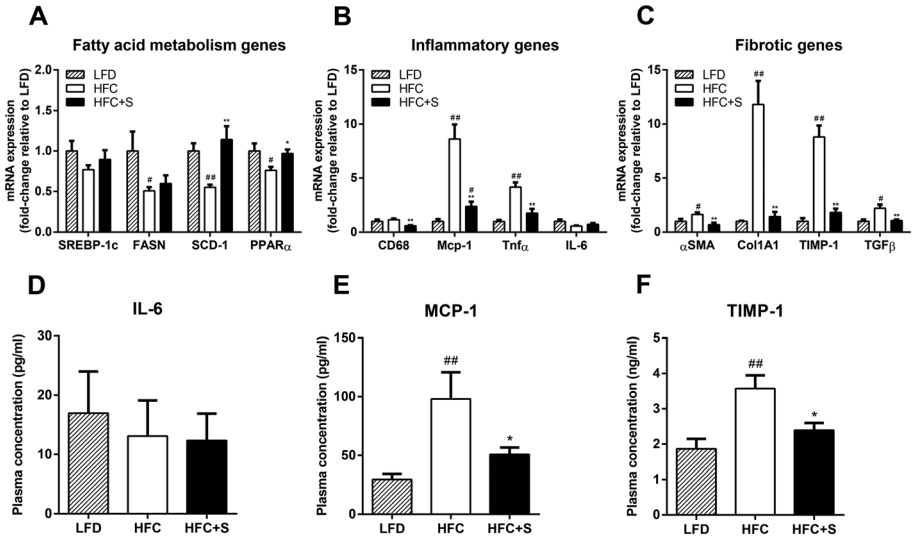

Figure 4

Gene expression of selected genes and plasma IL-6, MCP-1 and TIMP-1. The gene expression of selected genes involved in fatty acid metabolism (A), inflammation (B) or fibrosis (C) by RT-PCR of livers and plasma levels of IL-6 (D), MCP-1 (E) and TIMP-1 (F) of APOE*3Leiden.CETP mice fed a low-fat diet (LFD; $n = 5$), a high-fat/high-cholesterol diet (HFC; $n = 9$) or an HFC diet supplemented with salsalate (HFC + S; $n = 8$) for 12 weeks. *$P < 0.05$, **$P < 0.01$, significantly different from HFC; #$P < 0.05$, ##$P < 0.01$, significantly different from LFD; Mann-Whitney *U*-test.

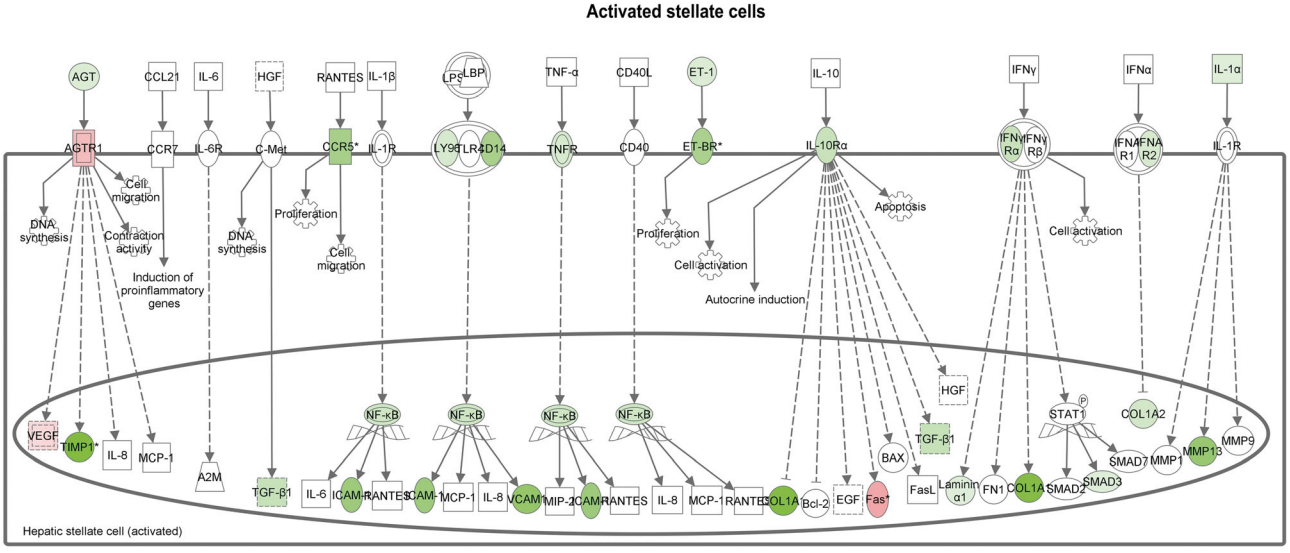

Figure 5

Hepatic fibrosis pathway analysis. Pathway analysis showing statistically significant gene expression changes in activated hepatic stellate cells of APOE*3Leiden.CETP mice fed a HFC diet supplemented with salsalate for 12 weeks ($n = 8$) relative to HFC diet fed control group ($n = 9$). Red colour indicates up-regulation, and green colour indicates down-regulation.

salsalate-treated group relative to the HFC group (with −87%, $P < 0.001$; Figure 6D). Twenty weeks of HFC feeding resulted in distinct fibrosis located in perisinusoidal/perivenular and periportal area (Figure 6A; Sirius Red staining). In all animals of both groups, at least some periportal and perisinusoidal fibrosis was seen (stage 2), but the extent of perisinusoidal fibrosis was profoundly reduced by salsalate treatment (4.1-fold decrease, $P < 0.01$; Figure 6E). We also analysed fibrosis quantitatively by measuring the ratio of hydroxyproline (as a measure for collagen) above proline (as a measure for total protein). The hydroxyproline/proline ratio was significantly lower (with 33%, $P < 0.01$) in the salsalate-treated group as compared with the HFC group (Fig. 6F). Collectively, these data demonstrated that salsalate was able to attenuate different aspects of NASH, that is, steatosis, inflammation and fibrosis.

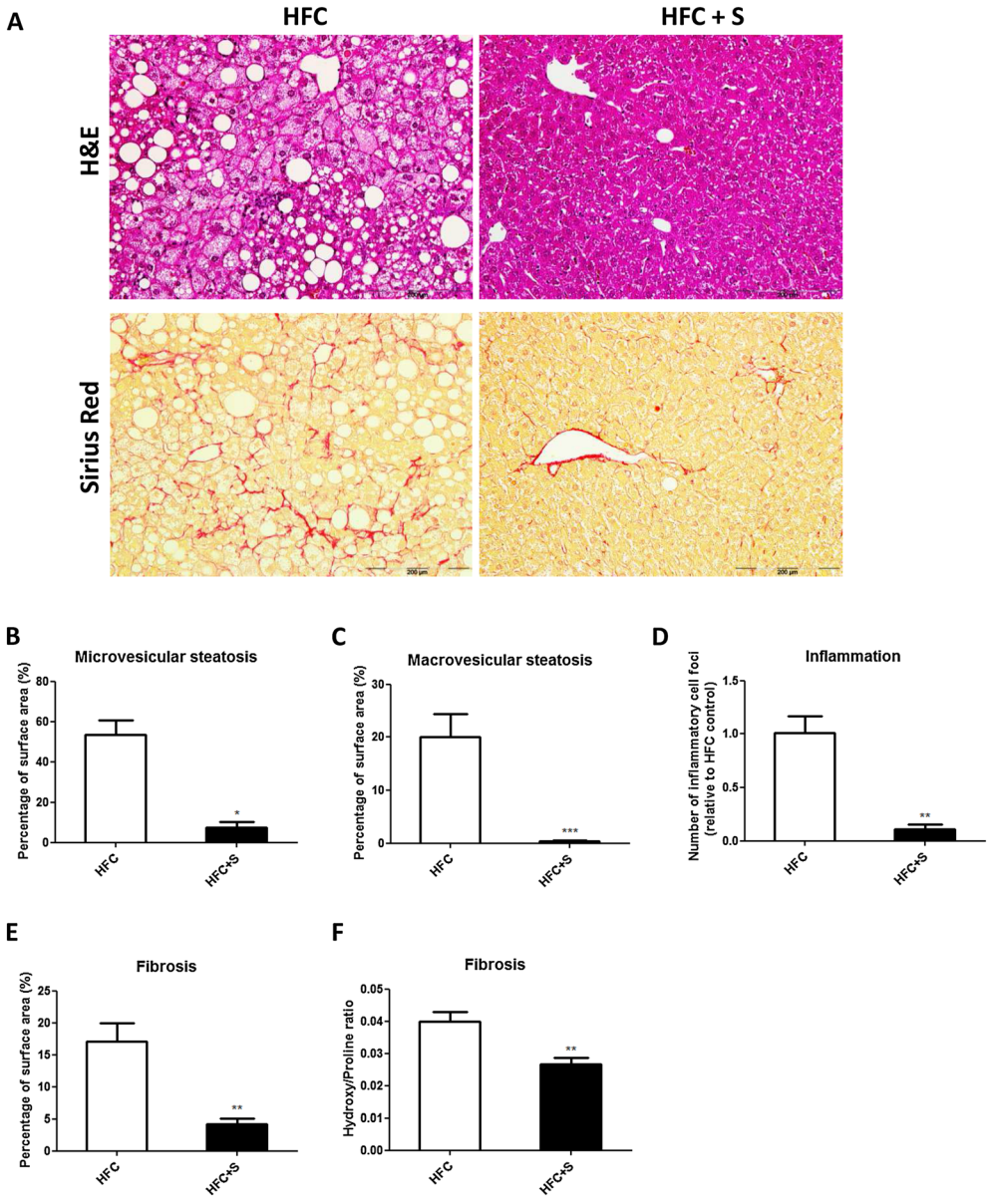

Figure 6

Histological photomicrographs and quantitative analysis of NASH in mice, treated for longer (20 weeks) with a lower dose of salsalate. Liver histological cross sections (A) and quantitative analysis (B–F) from APOE*3Leiden.CETP mice fed a high-fat and high-cholesterol diet (HFC; n = 12) or an HFC diet supplemented with salsalate (0.33% w/v; HFC + S; n = 8) for 20 weeks. Upper photomicrographs: haematoxylin and eosin (H&E); lower photomicrographs: Sirius Red staining; magnification 200×. Microvesicular (B) and macrovesicular (C) steatosis as percentage of total liver area, inflammatory foci per microscopic field (D), percentage perisinusoidal fibrosis (E) and the hydroxyproline ; proline ratio (F) were analysed. *$P < 0.05$, **$P < 0.01$, significantly different from HFC; ***$P < 0.001$, significantly different from HFC; Mann-Whitney U-test.

Discussion

In this study, we demonstrate for the first time that the treatment of obese, dyslipidemic and insulin-resistant E3L.CETP mice with salsalate markedly ameliorated diet-induced NASH and reduced the development of hepatic fibrosis. Bioinformatics analysis of the gene expression data identified regulatory pathways and upstream regulators in the liver that are specifically influenced by salsalate.

Surprisingly, hardly any preclinical or animal studies have been performed to evaluate the potential of salsalate as a treatment for NASH and liver fibrosis, although its utility in the prevention or management of a wide range of vascular disorders, including type 2 diabetes and metabolic syndrome, and NAFLD has been suggested before (McCarty, 2010; McCarty, 2011). Only one study showed that salsalate can ameliorate hepatic steatosis in rats that were fed a high-fat diet (Jung *et al.*, 2013). In this study, rats received a high-fat diet for 8 weeks, and the salsalate-treated group received salsalate mixed in the high-fat diet for an additional 6 weeks. The authors did not report whether inflammation was

induced by the diet or any anti-inflammatory effects of salsalate, but the duration of the diet was probably too short in this model to induce progression from NAFLD to NASH (Xu *et al.*, 2010). Our results corroborate these findings and confirm the beneficial effects of salsalate on steatosis. In addition, in our mouse model, we were able to model not only steatosis, dyslipidemia and insulin resistance but also hepatic inflammation and the natural progression of NASH to fibrosis, and we demonstrated the beneficial effects of salsalate on all these different aspects of NASH.

In humans, a dose of 3.0 $g \cdot day^{-1}$ is common for arthritis, and in the TINSAL-T2D trial, doses of 3.0, 3.5 and 4.0 $g \cdot day^{-1}$ were used. To translate the dosing used in our mouse studies with respect to the human dosing, the following simplified calculation can be used as a rough guide: 3–4 $g \cdot day^{-1}$ in a human of 75 kg would correspond with 40–60 $mg \cdot kg^{-1}$ per day, which would be equivalent to a dose of 400–600 $mg \cdot kg^{-1}$ per day in mice, when taking into account the approximately 10 times faster metabolism in mice (Reagan-Shaw *et al.*, 2008). In the first study, we used a 1% w/w dose and with mice weighing 29.8 g at the end of the experiment and a food intake of approximately 3.0 g per mouse per day. This protocol was equivalent to 1000 $mg \cdot kg^{-1}$ per day for the mouse. In the second experiment, we used one-third of the previous dose which would be equivalent to about 300 $mg \cdot kg^{-1}$ per day. The dose of the first experiment is therefore high in comparison with the human dose, while the dose of the second experiment is closer to the human dosage. Although the two doses were not compared, head-to-head, in the same experiment, we can nevertheless conclude that the lower dose also led to significant improvement in the different aspects of NASH (steatosis, inflammation and fibrosis) as well as some of the metabolic basal characteristics.

The mechanisms responsible for the beneficial metabolic effects of salsalate are not fully defined. The anti-inflammatory effects are believed to be attributable to inhibition of pro-inflammatory mediators such as the prostaglandins (Morris *et al.*, 1985), but also inhibition of neutrophil activation has been reported as an alternative mechanism (Altman, 1990). Inhibition of the NF-κB inflammatory pathway by salsalate has been shown in several rodent studies (Murthy *et al.*, 2010; Jung *et al.*, 2013) as well as in humans (Goldfine *et al.*, 2008). In addition, studies in humans have shown that salsalate can increase resting energy expenditure (Goldfine *et al.*, 2008; Meex *et al.*, 2011). Our data support the possibility that salsalate inhibits the NF-κB pathway and corroborate the increase in energy metabolism. Furthermore, our data revealed an important role for PPAR-α-mediated pathways with regard to the beneficial effects of salsalate on lipid metabolism.

Recent clinical studies have shown that salsalate improved inflammatory parameters, glycemic and insulin resistance in pre-diabetic and type 2 diabetic patients (Faghihimani *et al.*, 2012; Goldfine *et al.*, 2013b). Furthermore, a few clinical trials have been performed that investigated the effects of salsalate on vascular function (Goldfine *et al.*, 2013a), and currently, a clinical trial is being performed that is using salsalate to target inflammation in cardiovascular disease (TINSAL-CVD study). In the latter trial, salsalate will be given for 30 months to patients with cardiovascular disease. This trial is estimated to be completed in 2015 and will provide information of the effects of salsalate in relation to NAFLD/NASH as well, because as a secondary outcome measure, the effects of salsalate on fatty liver via computerized tomography and on levels of AST and ALT will be evaluated. Although the pleiotropic effects of salsalate, that is, anti-inflammatory effects and recently described beneficial effects on lipid and glucose metabolism, render salsalate an excellent candidate for treatment of NASH, not many designated clinical studies have been performed, which evaluate the potential beneficial effects of salsalate on NASH. To our knowledge, only one clinical study aiming to find effects of salsalate on NASH has been reported (Faghihimani *et al.*, 2013). In this study, salsalate did not change severity of fatty liver nor ALT and AST levels. However, the treatment period was short (1 month), and salsalate did not affect blood glucose and triglyceride levels, while other studies have reported significant decreases in plasma glucose and triglyceride levels upon salsalate treatment (Goldfine *et al.*, 2013a; Goldfine *et al.*, 2013b).

In summary, we reproduced NASH development with progression to fibrosis in HFC-fed E3L.CETP mice, a model that is characterized by obesity, metabolic anomalies and histopathological features similar to those observed in human NASH. In this model, salsalate exerted a preventive effect on the development of NAFLD and on the progression to steatohepatitis and fibrosis. We infer that salsalate may be pharmacologically useful for preventing the progression of steatohepatitis and fibrosis, and a promising therapeutic agent for human NASH. Further clinical studies are warranted to investigate the putative beneficial effects of salsalate on NASH in humans.

Acknowledgements

The authors gratefully acknowledge Erik Offerman and Frits van der Ham at TNO Metabolic Health Research for their help and technical assistance. The authors thank the TNO research programs 'Personalized Prevention and Therapy – Op Maat' and 'Enabling Technology Systems Biology' for supporting this study.

Author contributions

J. W. A. v. d. H., A. D. v. D., M. R. B., H. M. G. P., L. M. H., R. K. and A. M. v. d. H. contributed to conception and design. W. L., L. V., P. M. and J. V. collected the data. W. L., P. M., L. V., R. K. and A. M. v. d. H. analysed and interpreted the data. A. v. d. H. drafted the article. All authors critically revised the article for intellectual content. All authors approved the final version.

Conflict of interest

All authors have no conflict of interest.

References

Alexander SPH, Benson HE, Faccenda E, Pawson AJ, Sharman JL, Spedding M *et al* (2013). The Concise Guide to PHARMACOLOGY 2013/14: Nuclear Hormone Receptors. Br J Pharmacol 170: 1652–1675.

Altman RD (1990). Neutrophil activation: an alternative to prostaglandin inhibition as the mechanism of action for NSAIDs. Semin Arthritis Rheum 19: 1–5.

Bank RA, Krikken M, Beekman B, Stoop R, Maroudas A, Lafeber FP *et al.* (1997). A simplified measurement of degraded collagen in tissues: application in healthy, fibrillated and osteoarthritic cartilage. Matrix Biol 16: 233–243.

de Haan W, de Vries-van der Weij J, van der Hoorn JW, Gautier T, van der Hoogt CC, Westerterp M *et al.* (2008). Torcetrapib does not reduce atherosclerosis beyond atorvastatin and induces more proinflammatory lesions than atorvastatin. Circulation 117: 2515–2522.

Du P, Kibbe WA, Lin SM (2008). lumi: a pipeline for processing Illumina microarray. Bioinformatics 24: 1547–1548.

Faghihimani E, Amini M, Adibi A, Naderi Z, Toghiani A, Adibi P (2013). Evaluating the efficacy of salsalate on prediabetic and diabetic patients with fatty liver: a randomized clinical trial. J Res Pharm Pract 2: 40–43.

Faghihimani E, Aminorroaya A, Rezvanian H, Adibi P, Ismail-Beigi F, Amini M (2012). Reduction of insulin resistance and plasma glucose level by salsalate treatment in persons with prediabetes. Endocr Pract 18: 826–833.

Goldfine AB, Conlin PR, Halperin F, Koska J, Permana P, Schwenke D *et al.* (2013a). A randomised trial of salsalate for insulin resistance and cardiovascular risk factors in persons with abnormal glucose tolerance. Diabetologia 56: 714–723.

Goldfine AB, Fonseca V, Jablonski KA, Chen YD, Tipton L, Staten MA *et al.* (2013b). Salicylate (salsalate) in patients with type 2 diabetes: a randomized trial. Ann Intern Med 159: 1–12.

Goldfine AB, Fonseca V, Jablonski KA, Pyle L, Staten MA, Shoelson SE *et al.* (2010). The effects of salsalate on glycemic control in patients with type 2 diabetes: a randomized trial. Ann Intern Med 152: 346–357.

Goldfine AB, Silver R, Aldhahi W, Cai D, Tatro E, Lee J *et al.* (2008). Use of salsalate to target inflammation in the treatment of insulin resistance and type 2 diabetes. Clin Transl Sci 1: 36–43.

Jiang XC, Agellon LB, Walsh A, Breslow JL, Tall A (1992). Dietary cholesterol increases transcription of the human cholesteryl ester transfer protein gene in transgenic mice. Dependence on natural flanking sequences. J Clin Invest 90: 1290–1295.

Jung TW, Youn BS, Choi HY, Lee SY, Hong HC, Yang SJ *et al.* (2013). Salsalate and adiponectin ameliorate hepatic steatosis by inhibition of the hepatokine fetuin-A. Biochem Pharmacol 86: 960–969.

Kilkenny C, Browne W, Cuthill IC, Emerson M, Altman DG, NC3Rs Reporting Guidelines Working Group (2010). Animal research: reporting *in vivo* experiments: the ARRIVE guidelines. Br J Pharmacol 160: 1577–1579.

Kleiner DE, Brunt EM, Van Natta M, Behling C, Contos MJ, Cummings OW *et al.* (2005). Design and validation of a histological scoring system for nonalcoholic fatty liver disease. Hepatology 41: 1313–1321.

Koska J, Ortega E, Bunt JC, Gasser A, Impson J, Hanson RL *et al.* (2009). The effect of salsalate on insulin action and glucose tolerance in obese non-diabetic patients: results of a randomised double-blind placebo-controlled study. Diabetologia 52: 385–393.

Kramer A, Green J, Pollard J Jr, Tugendreich S (2014). Causal analysis approaches in Ingenuity Pathway Analysis. Bioinformatics 30: 523–530.

Kuhnast S, van der Hoorn JW, Pieterman EJ, van den Hoek AM, Sasiela WJ, Gusarova V *et al.* (2014). Alirocumab inhibits atherosclerosis, improves the plaque morphology, and enhances the effects of a statin. J Lipid Res 55: 2103–2112.

Liang W, Lindeman JH, Menke AL, Koonen DP, Morrison M, Havekes LM *et al.* (2014). Metabolically induced liver inflammation leads to NASH and differs from LPS- or IL-1beta-induced chronic inflammation. Lab Invest 94: 491–502.

McCarty MF (2011). Full-spectrum antioxidant therapy featuring astaxanthin coupled with lipoprivic strategies and salsalate for management of non-alcoholic fatty liver disease. Med Hypotheses 77: 550–556.

McCarty MF (2010). Salsalate may have broad utility in the prevention and treatment of vascular disorders and the metabolic syndrome. Med Hypotheses 75: 276–281.

McGrath JC, Drummond GB, McLachlan EM, Kilkenny C, Wainwright CL (2010). Guidelines for reporting experiments involving animals: the ARRIVE guidelines. Br J Pharmacol 160: 1573–1576.

Meex RC, Phielix E, Moonen-Kornips E, Schrauwen P, Hesselink MK (2011). Stimulation of human whole-body energy expenditure by salsalate is fueled by higher lipid oxidation under fasting conditions and by higher oxidative glucose disposal under insulin-stimulated conditions. J Clin Endocrinol Metab 96: 1415–1423.

Morris HG, Sherman NA, McQuain C, Goldlust MB, Chang SF, Harrison LI (1985). Effects of salsalate (nonacetylated salicylate) and aspirin on serum prostaglandins in humans. Ther Drug Monit 7: 435–438.

Murthy SN, Desouza CV, Bost NW, Hilaire RC, Casey DB, Badejo AM *et al.* (2010). Effects of salsalate therapy on recovery from vascular injury in female Zucker fatty rats. Diabetes 59: 3240–3246.

Pawson AJ, Sharman JL, Benson HE, Faccenda E, Alexander SP, Buneman OP *et al.* (2014). The IUPHAR/BPS Guide to PHARMACOLOGY: an expert-driven knowledge base of drug targets and their ligands. Nucl. Acids Res. 42: D1098–1106.

Reagan-Shaw S, Nihal M, Ahmad N (2008). Dose translation from animal to human studies revisited. FASEB J 22: 659–661.

Smyth GK (2004). Linear models and empirical bayes methods for assessing differential expression in microarray experiments. Stat Appl Genet Mol Biol 3: 1–25.

Tiniakos DG, Vos MB, Brunt EM (2010). Nonalcoholic fatty liver disease: pathology and pathogenesis. Annu Rev Pathol 5: 145–171.

van den Hoek AM, van der Hoorn JW, Maas AC, van den Hoogen RM, van Nieuwkoop A, Droog S *et al.* (2014). APOE*3Leiden.CETP transgenic mice as model for pharmaceutical treatment of the metabolic syndrome. Diabetes Obes Metab 16: 537–544.

van den Maagdenberg AM, Hofker MH, Krimpenfort PJ, de Bruijn I, van Vlijmen B, van der Boom H *et al.* (1993). Transgenic mice carrying the apolipoprotein E3-Leiden gene exhibit hyperlipoproteinemia. J Biol Chem 268: 10540–10545.

van der Hoogt CC, de Haan W, Westerterp M, Hoekstra M, Dallinga-Thie GM, Romijn JA *et al.* (2007). Fenofibrate increases HDL-cholesterol by reducing cholesteryl ester transfer protein expression. J Lipid Res 48: 1763–1771.

van der Hoorn JW, de Haan W, Berbee JF, Havekes LM, Jukema JW, Rensen PC *et al.* (2008). Niacin increases HDL by reducing hepatic expression and plasma levels of cholesteryl ester transfer protein

inAPOE*3Leiden.CETP mice. Arterioscler Thromb Vasc Biol 28: 2016–2022.

Verschuren L, Wielinga PY, Kelder T, Radonjic M, Salic K, Kleemann R, *et al*. (2014). A systems biology approach to understand the pathophysiological mechanisms of cardiac pathological hypertrophy associated with rosiglitazone. BMC Med Genomics 7: 35, 8794-7-35.

Westerterp M, van der Hoogt CC, de Haan W, Offerman EH, Dallinga-Thie GM, Jukema JW *et al*. (2006). Cholesteryl ester transfer protein decreases high-density lipoprotein and severely aggravates atherosclerosis in APOE*3-Leiden mice. Arterioscler Thromb Vasc Biol 26: 2552–2559.

Xu XM, Sansores-Garcia L, Chen XM, Matijevic-Aleksic N, Du M, Wu KK (1999). Suppression of inducible cyclooxygenase 2 gene transcription by aspirin and sodium salicylate. Proc Natl Acad Sci U S A 96: 5292–5297.

Xu ZJ, Fan JG, Ding XD, Qiao L, Wang GL (2010). Characterization of high-fat, diet-induced, non-alcoholic steatohepatitis with fibrosis in rats. Dig Dis Sci 55: 931–940.

Zadelaar S, Kleemann R, Verschuren L, de Vries-Van der Weij J, van der Hoorn J, Princen HM *et al*. (2007). Mouse models for atherosclerosis and pharmaceutical modifiers. Arterioscler Thromb Vasc Biol 27: 1706–1721.